Journal Pre-proof

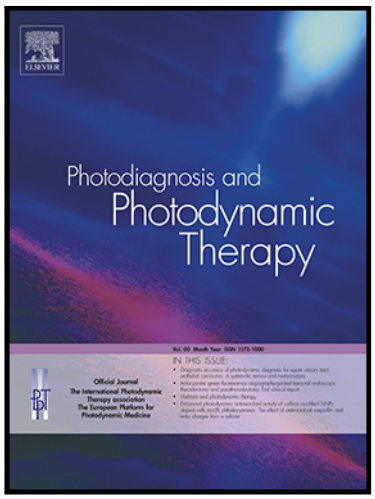

Sonodynamic Therapy with Chemo-Radiotherapy in High-Grade Brainstem Gliomas: A Prospective Phase IIa Clinical Trial

Xiaohao Liu , Linkuan Huangfu , Long Wang , Jiayin Ding , Tianqi Li , Yue Yu , Yahang Liu , Miaomiao Zhang , Zhifei Dai , Yingjuan Zheng

PII: S1572-1000(25)00827-0
DOI: https://doi.org/10.1016/j.pdpdt.2025.105296
Reference: PDPDT 105296

To appear in: *Photodiagnosis and Photodynamic Therapy*

Received date: 5 November 2025
Revised date: 21 November 2025
Accepted date: 21 November 2025

Please cite this article as: Xiaohao Liu , Linkuan Huangfu , Long Wang , Jiayin Ding , Tianqi Li , Yue Yu , Yahang Liu , Miaomiao Zhang , Zhifei Dai , Yingjuan Zheng , Sonodynamic Therapy with Chemo-Radiotherapy in High-Grade Brainstem Gliomas: A Prospective Phase IIa Clinical Trial, *Photodiagnosis and Photodynamic Therapy* (2025), doi: https://doi.org/10.1016/j.pdpdt.2025.105296

Highlights

- First prospective Phase IIa trial of sonodynamic therapy for brainstem glioma.
- A concurrent control group validates the additive benefit of sonodynamic therapy.
- SDT combined with chemo-radiotherapy shows favorable safety in HBSGs.
- SDT demonstrates a dose-dependent survival benefit for patients.

Title

Sonodynamic Therapy with Chemo-Radiotherapy in High-Grade Brainstem Gliomas：A Prospective Phase IIa Clinical Trial

Xiaohao Liu
Linkuan Huangfu
Long Wang
Jiayin Ding
Tianqi Li
Yue Yu
Yahang Liu
Miaomiao Zhang
Zhifei Dai
Yingjuan Zheng

Keywords Sonodynamic therapy· High-grade brainstem gliomas· Stupp regimen· Hematoporphyrin

Abstract

The treatment of high-grade brainstem gliomas (HBSGs), which are a type of malignant neoplasm, is challenging. There is a need to develop novel and effective therapeutic approaches for HBSGs. This study analyzed the data between sonodynamic therapy (SDT) group and control groups. 24 patients with HBSGs who were treated with the combination of SDT and Stupp regimen served as SDT group. Admitted patients (n = 39) during the same period in our hospital,receiving only the Stupp regimen served as the control group. Most SDT-related adverse events (AEs) were classified as grade 1–2, indicating manageable safety risks. The incidence rates of severe AEs were not significantly different between the two groups. The median progression-free survival (PFS) and overall survival (OS) were not significantly different between the SDT and control groups. However, the 6-month PFS rate (P = 0.009), 1-year PFS rate (P = 0.021), objective response rate(ORR) (P = 0.044), median duration of

disease control(DDC) (P = 0.002), median duration of response(DOR) (P = 0.010), and improvement in Karnofsky Performance Status(KPS) scores at month 1 post-treatment in the SDT group were significantly superior than those in the control group (P < 0.001). In the SDT group, the median OS of patients undergoing < 2 and ≥ 2 SDT cycles of treatment was 14.9 (95% CI: 6.9–22.9) and 20.9 months (95% CI: 16.5–25.3), respectively (P = 0.003). SDT and chemoradiotherapy combination was associated with favorable safety and dose-dependent survival benefit in patients with HBSGs, indicating its therapeutic potential.

Keywords

Sonodynamic therapy · High-grade brainstem gliomas · Stupp regimen · Hematoporphyrin · Chemotherapy · Radiation therapy

I. Introduction

High-grade brainstem gliomas (HBSGs), a type of malignant central nervous system tumors that originate from the brainstem, are challenging to treat as they are characterized by their unique anatomical location and highly invasive behavior, which contributes to poor prognosis [1]. Epidemiological studies have demonstrated that brainstem gliomas (BSGs) constitute approximately 10%–20% of all central nervous system tumors [2]. HBSGs (including subtypes, such as glioblastoma and anaplastic astrocytoma) account for approximately 20%–30% of all brainstem gliomas [3]. The peak incidence age of adult HBSGs is 40–60 years [4]. Low-grade brainstem gliomas are more prevalent in children. Meanwhile, HBSGs subtypes, such as diffuse intrinsic pontine gliomas (DIPGs), are malignant, adversely affecting pediatric patients [5][6].

Currently used therapeutic strategies for HBSGs are suboptimal. The brainstem comprises crucial nerve tracts, serving as the vital center of the human body. Thus, radical surgical resection of HBSGs is challenging [7].

Additionally, the poor prognosis of HBSGscan be attributed to their poor sensitivity to traditional radiotherapy and chemotherapy [8]. The overall survival (OS) of adult patients with HBSGs is only 9–12 months, while the 5-year survival rate is less than 5% [9]. In pediatric patients with DIPG, the median OS is approximately 9 months [10]. Advances in molecular pathology have improved our understanding of HBSGs' pathology. For example, adult HBSGs can be stratified according to the *IDH* mutation status. The identification of specific gene mutations, such as H3K27M in pediatric HBSGs, has provided new directions for precision diagnosis and therapy [11]. However, these advancements have not markedly improved the clinical outcomes of patients. Some exploratory clinical trials of targeted therapy and immunotherapy have been initiated [12][13] but are associated with limitations. The major limitations of HGBG treatment are the limited efficacy of targeted drugs and the development of drug resistance [14]. The limited clinical efficacy of therapeutics can be attributed to the blood-brain barrier (BBB), which restricts the efficiency of drug delivery [15]. Additionally, the enrollment rate of patients with HBSGs, especially pediatric patients, in clinical trials is low, delaying the development of novel treatment regimens.

Sonodynamic therapy (SDT), an emerging tumor treatment modality derived from photodynamic therapy (PDT), offers enhanced tissue penetration depth (> 10 cm) with minimal damage to healthy tissues due to the application of low-frequency ultrasound. Thus, SDT has potential therapeutic applications in deep-seated tumors [16]. The principle of SDT involves the selective accumulation of sonosensitizers in tumor tissues. The activation of sonosensitizers using low-intensity ultrasound (0.5–4.0 W/cm²) results in the generation of reactive oxygen species (ROS). ROS induce apoptosis by activating the mitochondrial (through the activation of cytochrome C release and caspase-9), death receptor (through caspase-8 activation), or endoplasmic reticulum stress pathways (through caspase-12 activation) [17][20]. Furthermore, SDT is reported to exert anti-angiogenic effects [21]. In BSGs, ultrasound can reversibly increase the permeability of the BBB [22][23] by decreasing the aggregation of

tight junction proteins (such as claudin-1 and claudin-5) in endothelial cells, which enhances drug delivery. These advantages highlight the therapeutic potential of SDT in brain tumor.

Based on previous preclinical studies and preliminary Phase I clinical trials [24][25], a prospective, single-center, single-arm phase IIa study was initiated to investigate the tolerability, safety, and efficacy of the combination of SDT and chemoradiotherapy in patients with HBSGs.

II. Methods

2.1 Study Subjects

2.1.1 Patient Source

This study was designed as a prospective, single-center, one-arm Phase IIa clinical trial. In this study, patients with HBSGs who received treatment at the First Affiliated Hospital of Zhengzhou University from January 2022 to January 2024 were recruited. The patients were screened according to the inclusion and exclusion criteria. A signed informed consent was obtained from eligible patients or their legal representatives. In this study, 24 patients were enrolled in the SDT group. Meanwhile, 39 patients with HBSGs who received the Stupp regimen alone during the same period in our hospital, served as the control group. Table S1 shows the detailed inclusion and exclusion criteria.

2.1.2 Ethical Approval

The study protocol was approved by the Ethics Committee of the First Affiliated Hospital of Zhengzhou University (project number: TA2022-145 and ethics approval number:L/G2022-K001-003). This study was performed according to the principles of the Declaration of Helsinki.

2.2 Research Methods

2.2.1 Therapeutic Drugs and Equipment

This trial used hematoporphyrin (trade name: *Xipofen*; Chongqing Mile Bio-pharmaceutical Co., Ltd) as the sonosensitizer. Hematoporphyrin is a porphyrin derivative that preferentially accumulates in tumor tissues. Upon activation by low-intensity ultrasound, it undergoes sonochemical reactions, primarily generating reactive oxygen species (ROS) such as singlet oxygen, which induces tumor cell death. Based on previous clinical data for PDT and SDT [24][26][28] and the drug instructions, the sonosensitizer was administered at a dose of 5 mg/kg body weight via intravenous infusion. The transcranial ultrasound therapy device (Model: 838D-M-L-Ⅱ) was purchased from Shijiazhuang Dokang Medical Equipment Co., Ltd. Previous experiments indicated that the sonodynamic effect of hematoporphyrin can be activated at an ultrasound intensity ≥ 0.5 W/cm² and a frequency of 800 kHz–1 MHz [29]. Ultrasound intensities of less than 5.8 W/cm² are reported to be safe for brain tissues [24][30]. Thus, the parameters for SDT were as follows: intensity: 1–1.25 W/cm²; frequency: 840 kHz; treatment duration: 60 min/session.

2.2.2 Study Design

Eligible candidates underwent maximal safe surgical tumor resection before participating in this study. The baseline tumor characteristics were assessed using magnetic resonance imaging (MRI) one week before treatment. All patients received the Stupp regimen [31]. Radiotherapy was initiated 4–6 weeks post-surgery with daily doses of 1.8–2.0 Gy administered 5 times weekly for 5–6 weeks (total dose: 45–60 Gy). All patients received volumetric modulated arc therapy (VMAT), with daily image-guided radiotherapy (IGRT) for precision. The clinical target volume (CTV) included the gross tumor volume (GTV), defined as the contrast-enhancing lesion on T1-weighted MRI plus any FLAIR hyperintensity deemed to represent tumor, with a 1–2 cm margin, adjusted for anatomical barriers. Concurrent temozolomide (TMZ) (75 mg/m^2/day) was administered for 42 days until radiotherapy completion. After a 4-week break, adjuvant chemotherapy was initiated in 28-day cycles (5 days on/23 days off).

The dosage used in the first cycle was 150 mg/m² /day for 5 days, while that used from the second cycle onward was 200 mg/m² /day for 5 days.

Tumor margins in patients belonging to the SDT group were delineated using MRI. The closest cranial projection area was selected for ultrasound transducer placement. After hair removal, the SDT target zone was marked. SDT was administered twice daily (6-hour intervals) for 5 successive days within each 28-day cycle synchronized with TMZ. Before treatment, a hematoporphyrin skin test was performed. If the patients tested negative in this test, they were intravenously infused with hematoporphyrin at a dose of 5 mg/kg body weight. SDT was initiated 40–48 hours post-infusion under light-protected conditions. Coupling gel was applied to the transducer for 60 min per target point. The treatment process is shown in Figure 1.

The half-life and clearance period of hematoporphyrin are 9.28 days and ≥ 2 months, respectively [32]. Consequently, patients were required to adhere to strict light avoidance measures. This included minimizing exposure to direct sunlight and bright indoor lights for at least one month post-treatment. Patients were advised to wear protective clothing, wide-brimmed hats, and UV-blocking sunglasses when outdoors. The precautions were gradually relaxed after one month, based on clinical assessment. To assess tumor response, cranial MRI examinations were performed at 4-week intervals. SDT was suspended in case of grade 3/4 hematological toxicity (possibly/definitely attributable to SDT).

2.2.3 Study Assessments

Primary endpoints: The primary outcomes of this study were the safety and tolerability of the SDT/chemoradiotherapy combination in patients with HBSGs. Patients in the SDT group underwent systematic prospective monitoring. The adverse events (AEs) in the control group were retrieved from routine clinical care records. All AEs were rigorously recorded based on subjective symptoms, objective physical examination findings,

clinical laboratory test results, and diagnostic imaging evaluations. The severity was classified according to the Common Terminology Criteria for AEs (CTCAE; version 5.0) established by the U.S. National Cancer Institute.

The secondary endpoints of this study were as follows: Progression-free survival (PFS), OS, and tumor response according to the Response Assessment in Neuro-Oncology criteria (RANO:version2.0) (complete response (CR), partial response (PR), stable disease (SD), and progressive disease (PD)). The objective response rate (ORR) was calculated as follows: ORR = CR + PR. The disease control rate (DCR) was calculated as follows: DCR = PR + CR + SD. The duration of disease control (DDC) spanned from first CR/PR/SD to PD/death, while the duration of response (DOR) spanned from first CR/PR to PD/death. Assessments were performed following the RANO: version2.0 criteria [33].

2.2.4 Data Analysis

Demographics, pretreatment history, pathology, Karnofsky Performance Status (KPS) scores, imaging data, and SDT parameters were analyzed. AEs were tabulated according to type/grade according to CTCAE (version 5.0). The data were censored if the endpoints were not met or patients were lost to follow-up (censoring time = last event-free observation).

Count data were reported as frequencies or percentages and compared using the chi-square test. Meanwhile, measurement data were compared using the independent t-test. Non-normally distributed/ordinal data were compared using the Mann-Whitney U test. The Kaplan-Meier survival curves were analyzed using the log-rank test. The risk factors for PFS or OS were identified using Cox regression (hazard ratios [HRs] + 95% confidence interval [CI]). Differences were considered significant at $P < 0.05$. All statistical analyses were performed using SPSS software (version 29.0) and R (version 4.2.3).

III. Results

3.1 Patient Baseline Characteristics

The last follow-up date was January 1, 2025. The median follow-up duration was 12.6 months (range: 3.2–29.6 months). The number of death cases in the SDT and control groups was 17 (70.8%) and 28 (71.8%), respectively. One patient was lost during follow-up in each group. . All patients in the SDT group received a minimum of one cycle of SDT (median number of cycles: 2 (range: 1–9)). Intergroup differences were not significantly different (Table 1). The optimal cutoff value for baseline tumor size was determined using receiver operating characteristic curve analysis. The area under the curve and optimal cutoff tumor size were 0.797 (95% CI: 0.680–0.913, $P < 0.001$) and 730 mm^2, respectively.

Table 1 Baseline Characteristics of Patients

Clinical Features [n, (%)]	DT (n = 24)	Control Group (n = 39)	*P*
Age			0.124
< 18	0 (41.7)	4 (61.6)	
≥ 18	4 (58.3)	5 (38.5)	
Sex			0.145
Male	5 (62.5)	7 (43.6)	
Female	(37.5)	2 (56.4)	
Surgical Intervention			0.939
Yes	(37.5)	5 (38.5)	
Grade			1.000
Grade 3	(12.5)	(15.4)	
Grade 4	9 (79.2)	9 (74.4)	

IDH			0.386
Wild-type	1 (87.5)	5 (89.7)	
Mutant	(4.2)	(0.0)	
H3K27M Mutation			0.336
Yes	(37.5)	0 (25.6)	
No	3 (54.2)	5 (64.1)	
H3K27me3			0.533
Loss	5 (62.5)	1 (53.8)	
Retained	(29.2)	4 (35.9)	
MGMT			1.000
Unmethylated	9 (79.2)	1 (79.5)	
Methylated	(12.5)	(10.3)	
KPS			0.836
< 70	(33.3)	4 (35.9)	
≥ 70	6 (66.7)	5 (64.1)	
Baseline Tumor Size			0.378
< 730 mm^2	0 (41.7)	2 (30.8)	
≥ 730 mm^2	4 (58.3)	7 (69.2)	
Tumor Location			0.605
Midbrain	4 (16.7)	(17.9)	
Pons	4 (58.3)	8 (46.2)	
Medulla	(25.0)	4 (35.9)	

SDT Cycles			NA
≤ 2	4 (58.3)	-	
> 2	0 (41.7)	-	

Baseline tumor size = product of the maximum perpendicular diameters of the tumor in the largest cross-section. Tumor location refers to the anatomical site of the largest cross-section.

3.2 Safety

AEs were categorized into the following three groups: (1) hematological toxicities (such as myelosuppression), gastrointestinal reactions, and liver injury associated with chemoradiotherapy; (2) intracranial edema-related side effects due to SDT and radiotherapy; (3) other random AEs. The most common AEs in the SDT and control groups were leukopenia, neutropenia, headache, and nausea/vomiting, which can be attributed to chemoradiotherapy-induced myelosuppression and increased intracranial pressure post-radiotherapy. The occurrence rate and severity of most AEs, including myelosuppression, gastrointestinal reactions, and liver injury, were not significantly different between the SDT and control groups. The incidence rate of grade 3 AEs, which manifested as leukopenia, elevated transaminases, and headache, was 3.8%. The grade 3 AE incidence rates were not significantly different between the SDT and control groups. Grade 4 or 5 AEs were not observed in the SDT and control groups (Table 2).

Table 2 Adverse Events in Different Groups

Adverse Event [n, (%)]	SDT (n = 24)		Control Group (n = 39)		*P*	
	All Grades	Grade 3-4	All Grades	Grade 3-4	All Grades	Grade 3-4

Leukopenia	21 (87.5)	1 (4.2)	36 (92.3)	5 (12.8)	0.528	0.256
Neutropenia	13 (54.2)	0	21 (53.8)	2 (5.1)	0.980	0.260
Thrombocytopenia	8 (33.3)	0	12 (30.8)	0	0.832	--
Lymphopenia	1 (4.2)	0	0	0	0.199	--
Anemia	10 (41.7)	0	21 (53.8)	0	0.348	--
ALT Increased	8 (33.3)	0	10 (25.6)	1 (2.6)	0.512	0.429
AST Increased	7 (29.2)	0	9 (23.1)	1 (2.6)	0.590	0.429
Hyponatremia	1 (4.2)	0	3 (7.7)	0	0.577	--
Hypokalemia	2 (8.3)	0	5 (12.8)	0	0.582	--
Hypermagnesemia	0	0	3 (7.7)	0	0.164	--
Dizziness	5 (20.8)	1 (4.2)	8 (20.5)	0	0.976	0.199
Headache	8 (33.3)	0	15 (38.5)	0	0.681	--
Seizure	6 (25.0)	1 (4.2)	6 (15.4)	0	0.345	0.199
Nausea/Vomiting	10 (41.7)	0	19 (48.7)	0	0.586	--
Diarrhea	0	0	1 (2.6)	0	0.429	--
Constipation	4 (16.7)	0	7 (17.9)	0	0.896	--
Fever	5 (20.8)	0	10 (25.6)	0	0.663	--
Fatigue	3 (12.5)	0	8 (20.5)	0	0.116	--
Rash	3 (12.5)	0	1 (2.6)	0	0.116	--
Blister	2 (8.3)	0	0	0	0.067	--
Burn	1 (4.2)	0	0	0	0.199	--
Hyperpigmentation	5 (20.8)	0	0	0	0.003	--

3.3 PFS Analysis

3.3.1 PFS Curves

The median PFS in the SDT (11.5 months; 95% CI: 6.3–16.8) was non-significantly higher than that in the control group (6.0 months; 95% CI: 4.4–7.6) (P = 0.077). The 6-month PFS rates in the SDT and control groups were 78.9% (70.5%–87.3%) and 48.7% (40.7%–56.7%), respectively (P = 0.009), while the 1-year PFS rates were 48.2% (37.8%–58.6%) and 19.9% (13.4%–26.4%), respectively (P = 0.021) (Fig. 2a).

3.3.2 Univariate and Multivariate Analysis of Prognostic Factors Associated with PFS

The baseline clinical characteristics of patients were subjected to univariate and multivariate Cox regression analyses to identify the effects of various factors on PFS(Table S2). Univariate analysis revealed that H3K27M mutation, H3K27me3, baseline KPS score, baseline tumor size, and number of SDT cycles were significantly associated with PFS. Multivariate analysis demonstrated that baseline tumor size and number of SDT cycles were independent prognostic factors for PFS (Table S2).

3.4 OS Analysis

3.4.1 OS Curves

The median OS in the SDT and control groups was 15.6 (95% CI: 12.7–18.5) and 10.8 months (95% CI:7.4–14.2), respectively (P = 0.400). Meanwhile, the 1-year OS rates in the SDT and control groups were 69.1% (95% CI: 59.3%–78.9%) and 47.9% (39.8%–56.0%) (P = 0.095), respectively (Fig.2b).

3.4.2 Univariate and Multivariate Analysis of Prognostic Factors Associated with OS

The factors affecting the OS were examined using univariate and multivariate Cox regression analyses (Table S3). Univariate analysis revealed that H3K27M, H3K27me3, baseline KPS score, baseline tumor size, and number of

SDT cycles were significantly associated with OS. Multivariate analysis demonstrated that baseline KPS score, baseline tumor size, and number of SDT cycles were independent prognostic factors for OS (Table S3).

3.5 Efficacy

Tumor response outcomes are summarized in Fig.2c and Fig.2d. Based on the RANO criteria, CR(Fig 3), PR, SD, and PD were achieved in 1, 7, 14, and 2 cases in the SDT group. Meanwhile, PR, SD, and PD were achieved in 4, 26, and 9 cases in the control group. Compared with those in the control group, the ORR was significantly higher (P = 0.044) and the DCR was not significantly different in the SDT group (P = 0.181) (Table 3).

Table 3 Tumor Response Evaluation in the Study Groups

Treatment Response Evaluation [n, (%)]	SDT	Control Group	*P*
CR	1 (4.2)	0	
PR	7 (29.2)	4 (10.3)	0.083
SD	14 (58.3)	26 (66.7)	
PD	2 (8.3)	9 (23.1)	
ORR (CR+PR)	8 (33.3)	4 (10.3)	**0.044**
DCR (CR+PR+SD)	22 (91.7)	30 (76.9)	0.181

Bold denotes statistical significance

Among patients without PD, the median DDC in the SDT and control groups was 10.1 (95% CI: 8.1–12.2) and 6.8 months (95% CI: 5.8–7.7), respectively (P = 0.002) (Fig.2 e), while the DOR (excluding SD/PD cases) was 10.1 (95% CI: 8.5–11.7) and 7.5 months (95% CI: 4.9–10.1) (P = 0.010), respectively. The DOR curve was

not plotted due to a limited number of CR/PR cases. The improvements in KPS scores at month 1 post-treatment in the SDT group were significantly superior to those in the control group ($P < 0.001$, Table 4).

Table 4 Changes in KPS Scores After Treatment

	SDT (n = 24)		Control Group (n = 39)		*P*
	Mean Rank	Rank Sum	Mean Rank	Rank Sum	
ΔKPS1	42.19	1012.50	25.73	1003.50	**< 0.001**
ΔKPS2	36.83	884.00	29.03	1132.00	0.075
ΔKPS6	35.08	842.00	30.10	1174.00	0.287

KPS1 = Change in KPS at month 1 post-treatment (KPS1 − Baseline KPS). KPS2 and ΔKPS6 represent changes at months 2 and 6, respectively. Bold denotes statistical significance

3.5.2 Effect of SDT Cycles on Survival

The median PFS and OS among patients undergoing ≤ 2 SDT treatment cycles were 8.4 (95% CI: 6.9–9.9 months) and 14.9 months (95% CI: 6.9–22.9 months), respectively, while those among patients undergoing > 2 SDT treatment cycles were 13.2 (95% CI: 11.5–14.9 months) and 20.9 months (95% CI: 16.5–25.3 months), respectively ($P = 0.037$ and 0.003 for PFS and OS, respectively) (Fig.2f–g).

Figure legends:

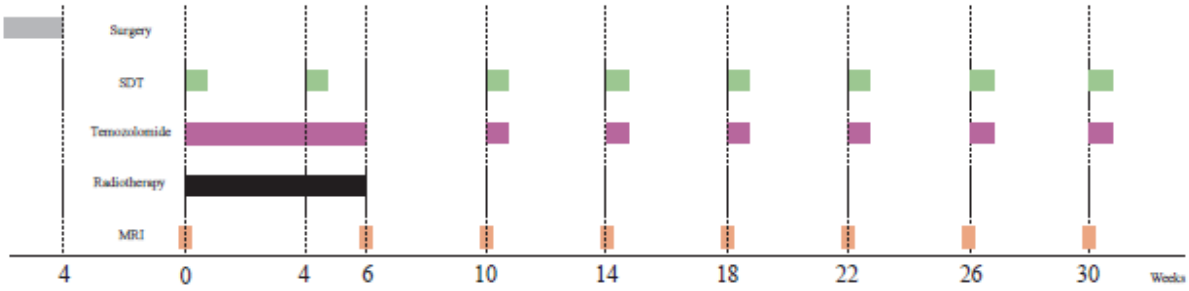

Fig. 1 Treatment flowchart. Maximal safe surgical tumor resection was done before participating in this study. SDT was administered 4 weeks post-surgery for twice daily for 5 successive days within each 28-day cycle. Radiotherapy was initiated 4 weeks post-surgery. Concurrent temozolomide was administered for 7 weeks until radiotherapy completion. Aafter a 4-week break, adjuvant chemotherapy was initiated in 28-day cycles. MRI examinations were performed at 4-week intervals

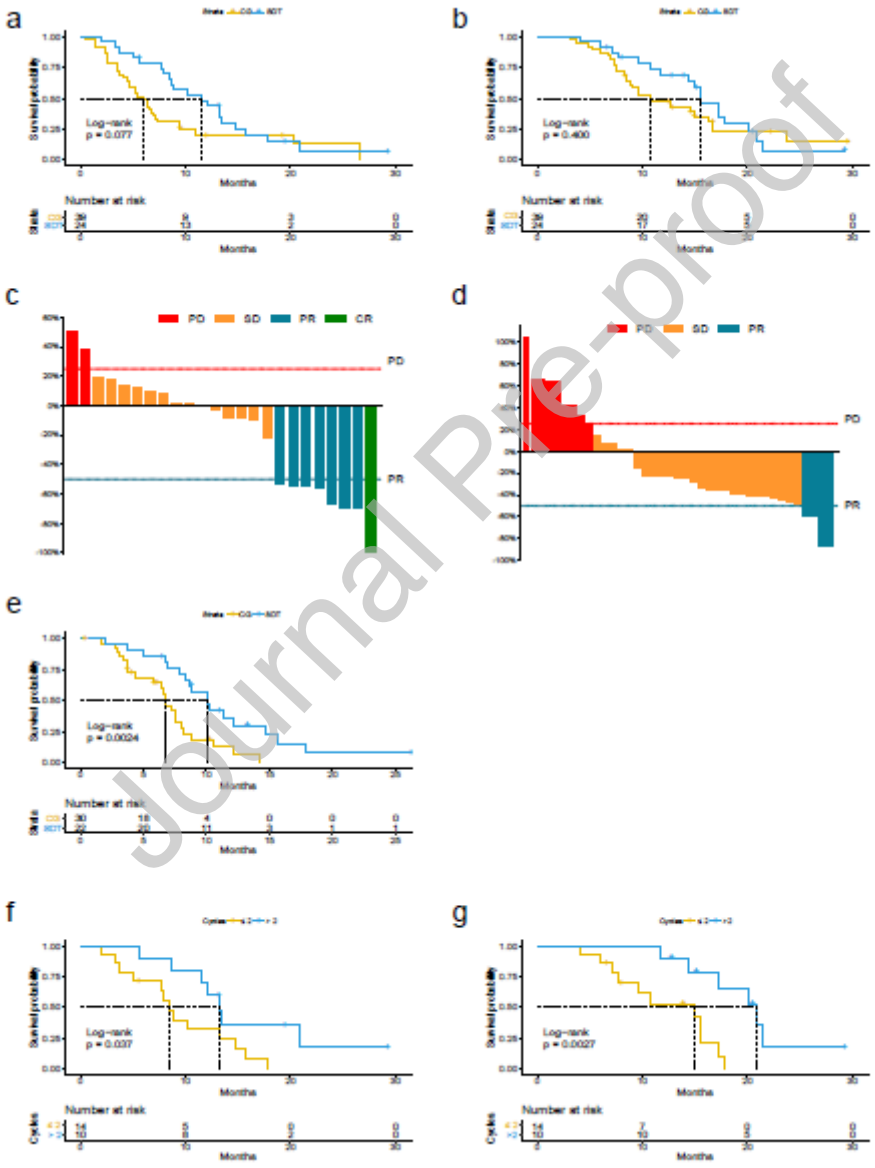

Fig. 2 Kaplan-Meier analysis of progression-free survival (PFS) between the sonodynamic therapy (SDT) and control groups (a). Kaplan-Meier analysis of overall survival (OS) between the SDT and control groups (b). Best treatment response in the SDT (c) and control groups (d). Kaplan-Meier analysis of duration of disease control (DDC) in the SDT and control groups (e). Kaplan-Meier analysis of (f) PFS and (g) OS in patients undergoing ≤ 2 and > 2 cycles of SDT. CG: Control group

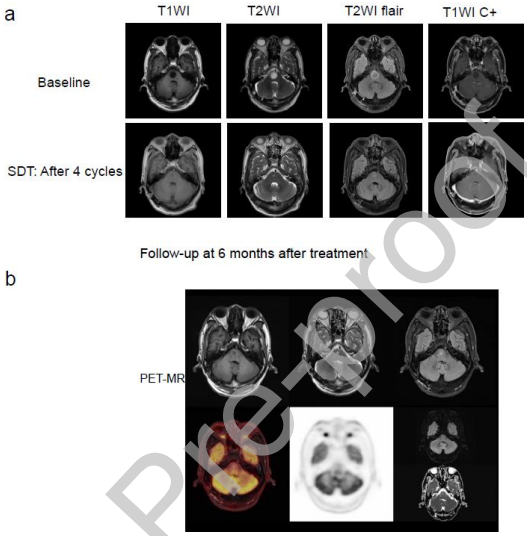

Fig. 3 MRI images of the CR patient :before the treatment; after 4 SDT cycles (a). PET-MR: follow-up at 6 months after treatment: there was no abnormal radioactive distribution in the brainstem (b)

IV. Discussion

HBSGs is a major health challenge in the field of neuro-oncology owing to their deep-seated anatomical location and aggressive behavior. Additionally, the BBB-mediated impairment of drug delivery further complicates HBSGs treatment. The currently employed standard treatment for HBSGs is the Stupp regimen (radiotherapy combined with TMZ). However, the median survival of patients with HBSGs is less than 12 months. Furthermore, effective therapeutic strategies are not available for recurrent cases [34]. Most clinical studies on HBSGs have not yielded favorable results. Izzuddeen et al. examined patients with DIPG who were treated with the combination

of TMZ and hypofractionated radiotherapy. This therapeutic regimen did not improve OS and was associated with hematological toxicity [35]. The combination of veliparib, TMZ, and radiotherapy did not improve the survival outcomes [36]. Immunotherapies, such as oncolytic virotherapy can potentially enhance the survival outcomes of these patients. However, these therapeutics are in the safety exploration phase [37].

SDT, a non-invasive modality that utilizes low-frequency ultrasound to activate sonosensitizers for ROS generation and enhance BBB permeability, has demonstrated favorable safety and efficacy in previous trials on recurrent glioblastoma and brain stem gliomas [24][25]. In our Phase I study (n = 11), the combination of SDT and radiotherapy achieved SD in 72.7% of patients with BSGs with no grade $\geqslant$ 3 treatment-related AEs and a PFS of 9.2 months, highlighting its potential clinical value. However, limitations, such as small sample size, heterogeneity in baseline patient characteristics, and delayed enrollment timing in the Phase I trial restricted the generalizability of efficacy. To address these limitations, this Phase IIa clinical trial was designed to expand the sample size, optimize treatment protocols (such as SDT cycle frequency and radiotherapy dose synchronization), and systematically evaluate the survival benefits and mechanistic synergies of the combination of SDT and chemoradiotherapy for HBSGs, providing evidence-based insights to inform subsequent investigations.

This is the first Phase IIa trial to investigate the therapeutic potential of the combination of SDT and chemoradiotherapy in HBSGs, integrating the targeted activation properties of SDT with conventional chemoradiotherapy. This study provides a non-invasive, comprehensive treatment strategy for HBSGs whose treatment is limited due to the BBB and surgical risks. This Phase IIa trial aimed to validate the safety and clinical translational value of hematoporphyrin-mediated sonodynamic and radiodynamic effects.

Safety assessments demonstrated excellent tolerability of hematoporphyrin at a dose of 5 mg/kg bodyweight with no dose-limiting toxicities. Most AEs were attributed to chemoradiotherapy-induced myelosuppression,

gastrointestinal disturbances, hepatotoxicity, and post-treatment cerebral edema. The incidence rates of these AEs were not significantly different between the SDT and control groups. Additionally, these AEs were predominantly mild (Grade 1–2) and can be effectively managed with supportive care. All SDT-related AEs (such as rash, blisters, burns, and pigmentation) were associated with inadequate light avoidance, with symptoms being mild and controllable. Notably, the incidence of headache was comparable between the SDT group (33.3%) and the control group (38.5%, P=0.681), and all reported headaches were Grade 1-2. This suggests that the SDT procedure itself, at the ultrasound parameters used, did not significantly contribute to or exacerbate headache beyond the baseline level expected from the underlying disease and concurrent radiotherapy. These findings confirm the favorable safety and tolerability profiles of the combination of SDT and chemoradiotherapy in HBSGs.

Preliminary efficacy observations revealed clinical symptom alleviation and tumor volume reduction in the SDT group. The PFS and OS were not significantly different between the control and SDT groups. However, the 6-month (78.9% vs 48.7%, $P = 0.009$) and 1-year PFS rates (48.2% vs 19.9%, $P = 0.021$) in the SDT group were higher than those in the control group, suggesting potential therapeutic benefits. The lack of significance in median PFS and OS can be attributed to limited sample size and potential type II error. Thus, these trends in survival outcomes must be confirmed in large cohorts. Patients undergoing > 2 cycles of SDT exhibited significantly higher PFS and OS than those undergoing ≤ 2 cycles of SDT. This suggests that an adequate number of SDT cycles can significantly improve prognosis. Standardized and full-course treatment should be ensured during therapy to enhance curative effects. Imaging assessments identified one patient achieving CR with near-total tumor regression and resolution of contrast-enhanced lesions on MRI, which was corroborated through metabolic imaging. In this study, seven patients attained PR. Compared with those in the control group, the ORR (33.3% vs 10.3%, $P = 0.044$), median DDC (10.1 vs 6.8 months, $P = 0.0007$), and DOR (10.1 vs 7.5 months, $P = 0.010$) were significantly higher in the SDT group.

Some cases in the SDT group exhibited significant clinical symptom alleviation during the initial phase of treatment. The improvements in KPS scores of patients in the SDT group at month 1 post-treatment initiation were markedly superior to those of patients in the control group. This phenomenon is uncommon in patients with HBSGs who previously received conventional radiotherapy and chemotherapy. In particular, one patient presented with dysphagia (cough while drinking water), emotional regulation disorders, and motor dysfunction (inability to stand independently) at baseline. After one cycle of SDT combined with radiotherapy and chemotherapy, improvements were observed in swallowing, emotional stability, and motor functions (standing for 3 minutes with supportive assistance). One patient with DIPG exhibited left-sided limb muscle weakness (grade III) and left oculomotor nerve palsy before treatment, which manifested as restricted eye movement and incomplete eyelid closure. After two cycles of combination therapy, the motor function significantly recovered, with limb muscle strength improving to grade IV and eye movement function nearly returning to physiological levels. However, this patient withdrew from subsequent treatment due to personal reasons, experienced disease progression three months after discontinuation, and passed away four months later. Although some patients in the SDT group did not meet the objective response criteria on imaging, their clinical symptoms (such as neurological deficits and symptoms of increased intracranial pressure) improved to varying degrees. This suggests that SDT may provide clinical benefits through unknown mechanisms, such as improving peritumoral circulation. Future studies should incorporate advanced methods, such as molecular imaging and biomarkers, to elucidate the underlying therapeutic mechanisms.

Compared with previously published SDT clinical trials, this study demonstrated differential advantages and mechanistic innovations. The Phase I/II clinical trial (NCT05362409) [38] conducted by Alpheus Medical, which employed the combination of 5-ALA and low-intensity diffused ultrasound for the treatment of recurrent high-grade gliomas, reported median OS and PFS of 15.7 and 5.5 months, respectively. The median OS in the SDT

group in this study was 15.6 months, which was similar to the results of the above-mentioned study but demonstraed significant improvements compared with below studies. Monje et al. conducted a Phase I clinical trial of panobinostat in pediatric patients with DIPG and reported that the median OS was 5.2 and 11.8 months in patients with PD and non-PD, respectively. The incidence rate of grade 3–4 hematological toxicity was 28% with one case of reversible encephalopathy [39]. Moraes et al. performed a retrospective cohort analysis of 253 patients with BSGs and revealed that the median OS was 11 months overall but was 10 months in pediatric patients (P = 0.002)[40]. In a Phase II randomized trial, Izzuddeen et al. compared the efficacy of the combination of hypofractionated radiotherapy (39 Gy/13 fractions) and TMZ with that of conventional radiotherapy (60 Gy/30 fractions) in DIPG. The hypofractionated + TMZ group had a median OS of 12 months, compared to 11 months in the conventional radiotherapy group (P=0.208). Median PFS was 8 vs. 7 months (P=0.198), respectively.. However, the incidence rate of grade 3–4 hematological toxicity in the hypofractionated radiotherapy +TMZ group was significantly higher than that in the conventional radiotherapy group (28% vs. 7%) [35]. These findings suggest that single-agent targeted therapy (e.g., panobinostat), conventional chemoradiotherapy, and optimized radiation fractionation do not overcome the survival bottleneck in BSGs and are associated with severe toxicity. In contrast, this study demonstrated a dual breakthrough through the synergistic effect of SDT + chemoradiotherapy. In particular, SDT + chemoradiotherapy improved survival outcomes (median OS reached 15.6 months, extending to 20.9 months in patients undergoing ≥ 2 SDT cycles). The observed dose-dependent effect provides a basis for clinical optimization. Additionally, SDT + chemoradiotherapy exhibited an enhanced safety profile. The incidence rate of grade 3–4 AEs was 3.8%, which was lower than that of hypofractionated RT + chemotherapy. Thus, this therapeutic regimen suppresses severe toxicities, such as myelosuppression.

Mechanistically, SDT has several advantages over traditional PDT. PDT cannot effectively treat deep-seated brain tumors due to limited light penetration depth (< 1 cm). In contrast, SDT can penetrate tissues deeper than 10 cm with the focusing properties of ultrasound, precisely acting on critical areas, such as the brainstem [41]. At the target area, ultrasound can activate the sonosensitizers (such as hematoporphyrin derivatives used in this study) to generate ROS. Singlet oxygen, a type of ROS, exerts cytotoxic effects on tumor cells [42][42]. In particular, singlet oxygen attacks subcellular organelles of tumor cells, such as the mitochondria and endoplasmic reticulum, disrupting cell metabolism and inducing apoptosis [43][44]. Additionally, SDT can reduce the aggregation of tight junction proteins (such as claudin-5) in the BBB through mechanical vibration, forming reversible pores with a diameter of approximately 100 nm and consequently enhancing the delivery efficiency of chemotherapeutic drugs (such as temozolomide). The drug concentration in tumor tissues of patients treated with SDT is 2–3 times higher than that in tumor tissues of patients treated with conventional treatment [45]. The ORR in the SDT (33.3%) group was significantly higher than that in the control group (10.3%, $P = 0.044$). This study also confirmed that SDT + chemoradiotherapy imparts dose-dependent survival benefits to patients with HBSGs who received more than two cycles of SDT. The median OS of patients undergoing ≥ 2 cycles of treatment (20.9 months) was significantly higher than that of patients undergoing ≤ two cycles (14.9 months ($P = 0.003$). This suggests that the anti-tumor effect of SDT may accumulate with the extension of treatment cycles. The underlying mechanisms may involve continuous remodeling of the tumor microenvironment, singlet oxygen accumulation, dynamic enhancement of BBB permeability, and progressive induction of immunogenic cell death [46][47][48].

This study has several limitations.Due to the low incidence of HGBGs, patient sample size was small, and the short follow-up period hindered comprehensive evaluation of long-term efficacy and survival benefits. The non-randomized design may have introduced selection bias (e.g., baseline KPS scores ≥ 70: SDT group: 66.7% vs control group: 64.1%), potentially affecting survival outcomes. To overcome this limitation, future studies must

perform propensity score matching. Additionally, systematic molecular profiling was not performed for all patients due to the limitations of single-center sample size and clinical resources, and research design prioritizing the verification of the feasibility of the treatment regimen. Furthermore, systematic molecular profiling was not listed as an endpoint. Multi-center studies integrating comprehensive molecular profiling should be conducted to establish a treatment decision-making system based on molecular characteristics. However, this study provides safety data and treatment references. Future research should verify the clinical value of SDT + chemoradiotherapy in HBSGs via multi-center, large-sample randomized clinical trials and explore novel sonosensitizers to optimize regimens.

V. Conclusions

The combination of SDT and chemoradiotherapy exhibited good safety and tolerability with controllable treatment-related AEs in patients with HBSGs. Additionally, this treatment combination improved patient prognosis in a dose-dependent manner.

Acknowledgements

We thank the patients and their families for participating in this study and for their efforts to cooperate with us in the follow-up.

Disclosure:

Funding The authors declare that no funds, grants, or other support were received during the preparation of this manuscript.

Data availability

The data that support the findings of this study are available from the corresponding author upon reasonable request.

Conflict of Interest

The authors have no relevant financial or non-financial interests to disclose.

Ethical Approval

The study protocol was approved by the Ethics Committee of the First Affiliated Hospital of Zhengzhou University (project number: TA2022-145 and ethics approval number:L/G2022-K001-003). This study was performed according to the principles of the Declaration of Helsinki.

Trial information: The trial was registered at the Chinese Clinical Trial Registry (http://www.chictr.org.cn/) (ChiCTR2200065992; November 2, 2022) .

Consent for Publication: The authors affirm that human research participants provided informed consent for publication.

Author Contributions

Xiaohao Liu: Conceptualization, Methodology, Investigation, Data Curation, Formal Analysis, Writing - Original Draft Preparation, Writing - Review & Editing.

Linkuan Huangfu: Methodology, Investigation, Resources, Data Curation, Validation.

Long Wang: Software, Validation, Formal Analysis, Visualization, Data Curation.

Jiayin Ding: Investigation, Resources, Data Curation.

Tianqi Li: Investigation, Resources.

Yahang Liu: Investigation, Resources.

Yue Yu: Investigation, Resources.

Miaomiao Zhang: Software, Formal Analysis, Visualization.

Zhifei Dai: Conceptualization, Resources, Writing - Review & Editing, Supervision, Project Administration.

Yingjuan Zheng: Conceptualization, Methodology, Resources, Writing - Review & Editing, Supervision, Project Administration, Funding Acquisition.

References

[1] Barbaro M, Fine HA, Magge RS. Scientific and Clinical Challenges within Neuro-Oncology. *World Neurosurg*. 2021;151:402-410. doi:10.1016/j.wneu.2021.01.151

[2] Liu H, Qin X, Zhao L, Zhao G, Wang Y. Epidemiology and Survival of Patients With Brainstem Gliomas: A Population-Based Study Using the SEER Database. *Front Oncol*. 2021;11:692097. Published 2021 Jun 11. doi:10.3389/fonc.2021.692097

[3] Eisele SC, Reardon DA. Adult brainstem gliomas. *Cancer*. 2016;122(18):2799-2809. doi:10.1002/cncr.29920

[4] Hanif F, Muzaffar K, Perveen K, Malhi SM, Simjee ShU. Glioblastoma Multiforme: A Review of its Epidemiology and Pathogenesis through Clinical Presentation and Treatment. *Asian Pac J Cancer Prev*. 2017;18(1):3-9. Published 2017 Jan 1. doi:10.22034/APJCP.2017.18.1.3

[5] Funakoshi Y, Hata N, Kuga D, et al. Pediatric Glioma: An Update of Diagnosis, Biology, and Treatment. *Cancers (Basel)*. 2021;13(4):758. Published 2021 Feb 12. doi:10.3390/cancers13040758

[6] Vanan MI, Eisenstat DD. Management of high-grade gliomas in the pediatric patient: Past, present, and future. *Neurooncol Pract*. 2014;1(4):145-157. doi:10.1093/nop/npu022

[7] Cohen KJ, Jabado N, Grill J. Diffuse intrinsic pontine gliomas-current management and new biologic insights. Is there a glimmer of hope?. *Neuro Oncol*. 2017;19(8):1025-1034. doi:10.1093/neuonc/nox021

[8] Zhang Y, Dong W, Zhu J, Wang L, Wu X, Shan H. Combination of EZH2 inhibitor and BET inhibitor for treatment of diffuse intrinsic pontine glioma. *Cell Biosci*. 2017;7:56. Published 2017 Oct 30. doi:10.1186/s13578-017-0184-0

[9] Champeaux Depond C, Bauchet L, Elhairech D, et al. Survival After Newly-Diagnosed High-Grade Glioma Surgery: What Can We Learn From the French National Healthcare Database?. *Brain Tumor Res Treat*. 2024;12(3):162-171. doi:10.14791/btrt.2024.0020

[10] Aziz-Bose R, Monje M. Diffuse intrinsic pontine glioma: molecular landscape and emerging therapeutic targets. *Curr Opin Oncol*. 2019;31(6):522-530. doi:10.1097/CCO.0000000000000577

[11] Killela PJ, Pirozzi CJ, Healy P, et al. Mutations in IDH1, IDH2, and in the TERT promoter define clinically distinct subgroups of adult malignant gliomas. *Oncotarget*. 2014;5(6):1515-1525. doi:10.18632/oncotarget.1765

[12] Cruz Da Silva E, Mercier MC, Etienne-Selloum N, Dontenwill M, Choulier L. A Systematic Review of Glioblastoma-Targeted Therapies in Phases II, III, IV Clinical Trials. *Cancers (Basel)*. 2021;13(8):1795. Published 2021 Apr 9. doi:10.3390/cancers13081795

[13] Giotta Lucifero A, Luzzi S. Against the Resilience of High-Grade Gliomas: The Immunotherapeutic Approach (Part I). *Brain Sci*. 2021;11(3):386. Published 2021 Mar 18. doi:10.3390/brainsci11030386

[14] Groenendijk FH, Bernards R. Drug resistance to targeted therapies: déjà vu all over again. *Mol Oncol*. 2014;8(6):1067-1083. doi:10.1016/j.molonc.2014.05.004

[15] Dong X. Current Strategies for Brain Drug Delivery. *Theranostics*. 2018;8(6):1481-1493. Published 2018 Feb 5. doi:10.7150/thno.21254

[16] Zhou LQ, Li P, Cui XW, Dietrich CF. Ultrasound nanotheranostics in fighting cancer: Advances and prospects. *Cancer Lett*. 2020;470:204-219. doi:10.1016/j.canlet.2019.11.034

[17] Dai S, Hu S, Wu C. Apoptotic effect of sonodynamic therapy mediated by hematoporphyrin monomethyl ether on C6 glioma cells in vitro. *Acta Neurochir (Wien)*. 2009;151(12):1655-1661. doi:10.1007/s00701-009-0456-5

[18] Wang P, Li C, Wang X, et al. Anti-metastatic and pro-apoptotic effects elicited by combination photodynamic therapy with sonodynamic therapy on breast cancer both in vitro and in vivo. *Ultrason Sonochem*. 2015;23:116-127. doi:10.1016/j.ultsonch.2014.10.027

[19] Liu Y, Wang P, Liu Q, Wang X. Sinoporphyrin sodium triggered sono-photodynamic effects on breast cancer both in vitro and in vivo [published correction appears in Ultrason Sonochem. 2022 Aug;88:106077. doi: 10.1016/j.ultsonch.2022.106077.]. *Ultrason Sonochem*. 2016;31:437-448. doi:10.1016/j.ultsonch.2016.01.038

[20] Dai S, Xu C, Tian Y, Cheng W, Li B. *In vitro* stimulation of calcium overload and apoptosis by sonodynamic therapy combined with hematoporphyrin monomethyl ether in C6 glioma cells. *Oncol Lett*. 2014;8(4):1675-1681. doi:10.3892/ol.2014.2419

[21] Song D, Yue W, Li Z, Li J, Zhao J, Zhang N. Study of the mechanism of sonodynamic therapy in a rat glioma model. *Onco Targets Ther*. 2014;7:1801-1810. Published 2014 Sep 30. doi:10.2147/OTT.S52426

[22] Kobus T, Vykhodtseva N, Pilatou M, Zhang Y, McDannold N. Safety Validation of Repeated Blood-Brain Barrier Disruption Using Focused Ultrasound. *Ultrasound Med Biol*. 2016;42(2):481-492. doi:10.1016/j.ultrasmedbio.2015.10.009

[23] Sheikov N, McDannold N, Sharma S, Hynynen K. Effect of focused ultrasound applied with an ultrasound contrast agent on the tight junctional integrity of the brain microvascular endothelium. *Ultrasound Med Biol*. 2008;34(7):1093-1104. doi:10.1016/j.ultrasmedbio.2007.12.015

[24] Zha B, Yang J, Dang Q, et al. A phase I clinical trial of sonodynamic therapy combined with temozolomide in the

treatment of recurrent glioblastoma. *J Neurooncol*. 2023;162(2):317-326. doi:10.1007/s11060-023-04292-9

[25] Huangfu L, Zha B, Li P, et al. A phase I clinical trial of sonodynamic therapy combined with radiotherapy for brainstem gliomas. Int J Cancer. 2025;156(5):1005-1014. doi:10.1002/ijc.35218

[26] Zhao Y, Tu P, Zhou G, et al. Hemoporfin Photodynamic Therapy for Port-Wine Stain: A Randomized Controlled Trial. *PLoS One*. 2016;11(5):e0156219. Published 2016 May 26. doi:10.1371/journal.pone.0156219

[27] Sun PH, Zhao X, Zhou Y, et al. Tolerance and pharmacokinetics of single-dose intravenous hemoporfin in healthy volunteers. *Acta Pharmacol Sin*. 2011;32(12):1549-1554. doi:10.1038/aps.2011.132

[28] Stylli SS, Howes M, MacGregor L, Rajendra P, Kaye AH. Photodynamic therapy of brain tumours: evaluation of porphyrin uptake versus clinical outcome. *J Clin Neurosci*. 2004;11(6):584-596. doi:10.1016/j.jocn.2004.02.001

[29] Zhou Q. Study on cavitation mechanism and acoustic field optimization of porphyrin derivative-mediated sonodynamic therapy[D]. Doctoral dissertation. Harbin: Harbin Institute of Technology; 2022.（In Chinese）

[30] Sarica C, Nankoo JF, Fomenko A, et al. Human Studies of Transcranial Ultrasound neuromodulation: A systematic review of effectiveness and safety. *Brain Stimul*. 2022;15(3):737-746. doi:10.1016/j.brs.2022.05.002

[31] Stupp R, Mason WP, van den Bent MJ, et al. Radiotherapy plus concomitant and adjuvant temozolomide for glioblastoma. N Engl J Med. 2005;352(10):987-996. doi:10.1056/NEJMoa043330IF: 96.2 Q1

[32] Bellnier DA, Greco WR, Loewen GM, Nava H, Oseroff AR, Dougherty TJ. Clinical pharmacokinetics of the PDT photosensitizers porfimer sodium (Photofrin), 2-[1-hexyloxyethyl]-2-devinyl pyropheophorbide-a (Photochlor) and 5-ALA-induced protoporphyrin IX. *Lasers Surg Med*. 2006;38(5):439-444. doi:10.1002/lsm.20340

[33] Wen PY, Macdonald DR, Reardon DA, et al. Updated response assessment criteria for high-grade gliomas: response assessment in neuro-oncology working group. *J Clin Oncol*. 2010;28(11):1963-1972. doi:10.1200/JCO.2009.26.3541

[34] Komotar RJ, Otten ML, Moise G, Connolly ES Jr. Radiotherapy plus concomitant and adjuvant temozolomide for glioblastoma-a critical review. *Clin Med Oncol*. 2008;2:421-422. doi:10.4137/cmo.s390

[35] Izzuddeen Y, Gupta S, Haresh KP, et al. Hypofractionated radiotherapy with temozolomide in diffuse intrinsic pontine gliomas: a randomized controlled trial[J]. J Neurooncol. 2020, 146(1):91-95

[36] Baxter PA, Su JM, Onar-Thomas A, et al. A phase I/II study of veliparib (ABT-888) with radiation and temozolomide in newly diagnosed diffuse pontine glioma: a Pediatric Brain Tumor Consortium study[J]. Neuro Oncol. 2020, 22(6):875-

[37] Gállego Pérez-Larraya J, Garcia-Moure M, Labiano S, et al. Oncolytic DNX-2401 Virus for Pediatric Diffuse Intrinsic Pontine Glioma[J]. N Engl J Med. 2022, 386(26):2471-2481

[38] Alpheus Medical. "Positive Results from Phase I/II Clinical Trial of Alpheus' Sonodynamic Therapy for Recurrent High-Grade Glioma." Presented at the 29th Annual Meeting of the Society for Neuro-Oncology, Houston, Texas, USA, November 21-24, 2024.

[39] Monje M, Cooney T, Glod J, et al. Phase I trial of panobinostat in children with diffuse intrinsic pontine glioma: A report from the Pediatric Brain Tumor Consortium (PBTC-047). Neuro Oncol. 2023;25(12):2262-2272. doi:10.1093/neuonc/noad141

[40] Moraes FY, Gouveia AG, Marta GN, Viani GA. Radiotherapy combined or not with chemotherapy in adult or pediatric patients with brainstem glioma: a population-based study. Rep Pract Oncol Radiother. 2023;28(2):181-188. Published 2023 Jun 26. doi:10.5603/RPOR.a2023.0016

[41] Scanlon SE, Shanahan RM, Bin-Alamer O, et al. Sonodynamic therapy for adult-type diffuse gliomas: past, present, and future. *J Neurooncol*. 2024;169(3):507-516. doi:10.1007/s11060-024-04772-6

[42] Cheng D, Wang X, Zhou X, Li J. Nanosonosensitizers With Ultrasound-Induced Reactive Oxygen Species Generation for Cancer Sonodynamic Immunotherapy. *Front Bioeng Biotechnol*. 2021;9:761218. Published 2021 Sep 30. doi:10.3389/fbioe.2021.761218

[43] Li YH, Jia HR, Wang HY, Hua XW, Bao YW, Wu FG. Mitochondrion, lysosome, and endoplasmic reticulum: Which is the best target for phototherapy?. J Control Release. 2022;351:692-702. doi:10.1016/j.jconrel.2022.09.037

[44] Ma J, Yuan H, Zhang J, et al. An ultrasound-activated nanoplatform remodels tumor microenvironment through diverse cell death induction for improved immunotherapy. *J Control Release*. 2024;370:501-515. doi:10.1016/j.jconrel.2024.05.001

[45] Chen J, Zhou Q, Cao W. Multifunctional Porphyrin-Based Sonosensitizers for Sonodynamic Therapy[J]. Advanced Functional Materials, 2024, 34(40): 2405844.

[46] Zhang Q, Bao C, Cai X, et al. Sonodynamic therapy-assisted immunotherapy: A novel modality for cancer treatment. *Cancer Sci*. 2018;109(5):1330-1345. doi:10.1111/cas.13578

[47] Ji C, Si J, Xu Y, et al. Mitochondria-targeted and ultrasound-responsive nanoparticles for oxygen and nitric oxide codelivery to reverse immunosuppression and enhance sonodynamic therapy for immune activation. *Theranostics*. 2021;11(17):8587-8604. Published 2021 Jul 25. doi:10.7150/thno.62572

[48] Zhou Y, Jiao J, Yang R, et al. Temozolomide-based sonodynamic therapy induces immunogenic cell death in glioma. *Clin Immunol*. 2023;256:109772. doi:10.1016/j.clim.2023.109772

List of Supporting Information:

Table S1 Inclusion and exclusion criteria

Table S2 Univariate and Multivariate Cox Regression Analysis of PFS-Related Factors

Table S3 Univariate and Multivariate Cox Regression Analysis of OS-Related Factors